Supplementary material

Activatable Naphthalimide-Based Fluorescent Probe for Hydrogen Peroxide Detection: Visualizing Microcystin-LR Induced Oxidative Stress in Zebrafish and Hepatocyte Injury Mechanism

Linmin Nie[1], Ruiqin Zhang[1], Suyu Liu[1], Kexin Mu[1], Tingting Zhao[1], Xueping Hu[1]*, Xingliang Song[1]* Xiaohong Liu[1], Xueyong Jin[1], Xiaoyan Wang[4], Yan Huang[4], and Lingxin Chen[2,3]*

[1] *School of Chemistry and Chemical Engineering, Linyi University, Linyi 276005, P.R. China.* E-mail: huxueping@lyu.edu.cn (X. Hu); songxingliang@lyu.edu.cn (X. Song)

[2] Shandong Key Laboratory of Coastal Zone Environmental Processes and Ecological Security, Shandong Engineering Research Center for Coastal Zone Ecological & Environmental Monitoring Technologies and Equipment, Yantai Institute of Coastal Zone Research, Chinese Academy of Sciences, Yantai 264003, China. E-mail: lxchen@yic.ac.cn (L. Chen)

[3] College of Chemistry and Chemical Engineering, Institute for Advanced Study, Shaoxing University, Shaoxing 312000, China

[4]School of Pharmacy, Shandong Medical and Pharmaceutical University, Yantai 264003, China

---

***Corresponding author**

E-mail: lxchen@yic.ac.cn (L. Chen); huxueping@lyu.edu.cn (X. Hu); songxingliang@lyu.edu.cn (X. Song)

Table of Contents

Table S1. Atomic orbital HOMO-LUMO compositions of compounds

Text 1. Chemicals and materials

Fluorescence spectra were acquired on a F-4700 Spectrophotometer. High-resolution mass spectra (HRMS) were acquired using a Q-Ex active Focus. Nuclear Magnetic Resonance (NMR) data were collected on an Agilent JNM-ECZL400S mass spectrometer. Cellular and zebrafish imaging were performed through a laser scanning confocal microscopy (AI+ Cell Manipulator Plus). The pH data were acquired from a PHS-3 C Precision pH/mV Meter.

All chemicals in this study were analytical/spectroscopic grade and purchased from commercial suppliers. 4-bromo-1,8-naphthalenedicarboxylic anhydride, 2-(2-aminoethoxy)ethanol, bis(pinacol)diboron, potassium acetate, Pd(dppf)Cl_2, 1,4-dioxane, N,N-Dimethylformamide, 30% H_2O_2, potassium carbonate and 4-Bromomethylphenylboronic acid ester.

Text 2. Endogenous H_2O_2 imaging in zebrafish：

Normal 5-day-old zebrafish were used for bioimaging experiments. The zebrafish were cultured in E3 medium in a standardized incubator at 28 °C. First, zebrafish were incubated with Probe A for 30 min, serving as the control group. In the experimental groups, zebrafish were first incubated with 10 μL Probe A for 30 min, then divided into 3 groups: they were incubated with 1.5 μg/L mc-LR for different time periods (20 min, 40 min, 60min and 80 min), followed by washing 3 times with PBS solution. Glycerol was used to fix live zebrafish for imaging.

Text 3 Method for preparing garlic extract:

Take fresh garlic (25g), peel it, slice thinly, and grind thoroughly into powder in a mortar. Transfer the powder to a 10 mL centrifuge tube, add an appropriate amount of distilled water, and centrifuge at 8000 rpm for 5 minutes using a high-speed refrigerated centrifuge. After centrifugation, collect the supernatant by decanting (discarding the precipitate). Take commercial fish feed and fully immerse it in the prepared garlic supernatant. Soak at room temperature for 24 hours to ensure complete adsorption of garlic juice components. After soaking, transfer the garlic-adsorbed fish feed to a freeze

dryer. Process by freeze drying until constant weight is achieved, yielding garlic-containing powdered fish feed. [1]

In the mass spectrometry analysis of garlic saponin samples, due to the strong affinity of the garlic saponin molecule to cations, the main components were well separated in the combined electrospray mass spectrometry positive ion detection map. As can be seen from the **Figure S13**, excimer ion peaks such as 1243 [M H] and 1283 [M Na H_2O] can be observed in the primary mass spectrometry, but the ion peaks of different saponin molecules combined with molecules are different. The molecular ion peaks are 1243 [M H], the base peaks are 757 [M H-3×162], the others are 1081 [M H-162] and 595 [M H-4×162], and 595 [M H-4×162] and 433 [M H-5×162] in secondary mass spectrometry 757. $[M+H]^+$ (m/z 1243) ions lose a series of glucose-based glycan fragments (each with a mass of 162) sequentially under collision-induced dissociation, resulting in a molecular weight of 1242 for the compound. Secondary mass spectra 595 contain m/z values of 271, 289, 253, and 432, the m/z value of 432 corresponds to the molecular weight of this saponin. Preliminary inferences suggest that the possible structures are as shown in **Figure S14**.

Text 4 Different routes of probe a synthesis:

1,8-Naphthalimide probe is selected as an excellent fluorescent matrix because of its low price, easy modification of structure and high fluorescence quantum yield. [2] Initially, the probe intermediate was generated by nucleophilic substitution reaction between 4-bromo-1,8-naphthalic anhydride and diethylene glycol amine, and the probe A was generated by Suzuki-Miyaura coupling reaction between the intermediate and palladium dichloride. However, the borate group on the probe A is easy to hydrolyze, which makes it difficult to detect hydrogen peroxide next. The second design is to hydrolyze the probe, and by introducing phenylborate as the recognition group, it can realize good specific recognition of hydrogen peroxide. When the probe reacts with hydrogen peroxide, phenylborate is partially oxidized to phenolic hydroxyl. It has excellent specific selectivity and good biocompatibility. The detailed information can be found in **Figure S12**.

Text 5. Quantum chemical studies:

All theoretical calculations were implemented by density functional theory (DFT) method on the Gaussian 09 program. The 6-31G** basis set was assigned for the main group elements. Geometry optimization of the ground state structures was carried out with DFT at the B3LYP level. The optimizations of A, A_2, A_3, B and B_1 compound were determined based on the energy-minimized structures, the molecular structures are shown in **Figure S12**. Moreover, the Atomic Orbital HOMO-LUMO Compositions of these Compounds shown in **table S1.**

Quantum chemical calculations [3] were employed to analyze the frontier molecular orbital (FMO) properties of the newly designed probe (**Compound A**) and a series of reference compounds, providing key insights into their electronic structures, reactivity, and potential biological activity. Frontier molecular orbital analysis, centered on the highest occupied molecular orbital (HOMO) and lowest unoccupied molecular orbital (LUMO), is crucial for evaluating molecular interactions with biological targets. The energy gap (ΔE) between these orbitals directly correlates with chemical reactivity and biological activity characteristics. For the newly designed probe **(Compound A)**, calculations yielded a HOMO energy of -7.56 eV and a LUMO energy of -1.56 eV, resulting in a HOMO-LUMO energy gap (ΔE) of 6.00 eV. Notably, the probe A'HOMO is predominantly localized to the two benzene rings of naphthylimide moiety, while the LUMO is concentrated in the naphthylimide core. This spatial distribution of frontier molecular orbitals indicates that the naphthoylimide unit serves as the primary structural element involved in molecular interactions, potentially underpinning its specific target-directed biological activity. This characteristic may underpin its target-specific biological activity. Compared to (**Table S1**), the HOMO-LUMO energy gaps of the reference compounds are slightly higher, ranging from 6.02 to 6.07 eV. For example, **Cmpound A_3** exhibits a HOMO energy of -7.66 eV, a LUMO energy of -1.63 eV, and a ΔE of 6.03 eV; **Cmpound A_2** has a HOMO energy of -7.80 eV, a LUMO energy of -1.78 eV, and a ΔE of 6.02 eV; **Compound B** has a HOMO energy of -7.81 eV and a LUMO energy of -1.76 eV, yielding ΔE = 6.05 eV; **Compound B_1** has a HOMO energy of -7.93 eV and a LUMO energy of -1.86 eV, yielding ΔE = 6.07 eV. The slightly larger bandgap of the reference compounds implies lower electron delocalization and potentially reduced reactivity compared to the newly designed probes.

Furthermore, the spatial distribution of the frontier molecular orbitals in the reference compounds

differs from that in the designed probes. In some reference compounds, the HOMO and LUMO are primarily confined to the naphthylimide ring, suggesting only this core participates in interactions with charged biological ions. This contrasts with the designed probes, whose frontier molecular orbitals span in the naphthylimide rings, indicating broader and potentially target-specific interaction characteristics. In case of **Compound A**, both HOMO and LUMO are fastened on naphthalimide ring, inferring that only naphthalimide ring interacts with charged ions, indicating the importance of naphthalimide for bioactivity.

Text 6. Effect of probe A on the survival of HeLa cells:

Add 100 μL of cell suspension to each well of a 96-well cell culture plate. Three to five holes are set in each group, and 100 μL PBS is added in the peripheral holes to eliminate the edge effect. The 96-well plate was incubated in a 5% CO_2 incubator at 37 ℃ for 24 hours, and then the cell adhesion and growth were observed under an inverted microscope. Discard the original medium in the 96-well plate. In the experimental group, 100 μL drug-containing medium (concentration: 5 μmol/L, 10, 15) was added to each well; The blank group was added with 100 μL drug-free medium. Continue to cultivate in a 5% CO_2 incubator at 37 ℃. After the incubation, add 10 μL CCK-8 [4] to each well, gently shake the 96-well plate to fully mix the reagents, incubate in the incubator for 1 hour, and detect the absorbance at 450 nm with enzyme-labeled instrument. Detailed cell survival rate-concentration curves are shown in **Figure S9**.

Text 7. Confocal fluorescence microscopic images of HeLa cells：

HeLa cells were cultured in DMEM medium containing 10 % fetal serum in 37 ℃ and 5 % CO_2 incubator. HeLa cells were replaced with fresh medium 2-3 times a day, passaged at a ratio of 1:2, and digested with trypsin at room temperature for 2-3 min. HeLa cells were incubated with probe A (10 μmol/L) for 30 min, washed with PBS solution for 2-3 times and then divided into 4 groups: treated with 1.5 μmol/L, 10.5 μmol/L, 15 μmol/L and 90 μmol/L hydrogen peroxide for 30 min, respectively.

Text 8. Molecular docking analysis:

The optimal molecular docking conformation of the small molecule with the zebrafish transporter. [5]From the spatial distribution characteristics, it can be seen that the small molecule is located within a relatively enclosed binding site inside the zebrafish transporter. This site is formed by the amino acids Asp189, Asp188, Met180, Tyr199, Arg192, Leu202, Phe198, Glu176, Val179, Ser191, Gly183, Asn195 from the B chain, along with Lys30 from the A chain and Tyr554, Leu558 from the E chain. Analysis of interactions at the binding interface indicates that interactions between the small molecule and the protein are primarily noncovalent. Specifically, the small molecule forms five sets of hydrogen bonds with residues Asn195 (B), Gly183 (B), Ser191 (B), Asp189 (B), and Asp188 (B). These directed interactions enhance the stability of molecular recognition to a certain extent. Simultaneously, the hydrophobic structural regions within the small molecule's backbone form tight hydrophobic contacts with multiple residues including Tyr554 (E), Met180 (B), and Lys30 (A). This facilitates the exclusion of water molecules from the binding site, further stabilizing the complex structure. The combined presence of these diverse interactions enables the small molecule to maintain a relatively stable binding state within the zebrafish transporter binding pocket.

Text 9. Confocal fluorescence image：

The liver was dissected from the fish body and immersed in 4 % paraformaldehyde for 24 - 48 h. Subsequently, it was immersed in 15 % sucrose solution until it sank to the bottom, and then replaced with 30 % sucrose solution for overnight immersion. First, the fish liver was incubated with Probe A for 1 h, then treated with 1.5 μmol/L H_2O_2 (a_2-c_2), 10.5 μmol/L H_2O_2 (a_2-c_2), and 90 μmol/L H_2O_2 (a_2-c_2) for 30 min, respectively.

Text 10. Confocal fluorescence microscopic images of zebrafish

Normal 5-day-old zebrafish were selected for bioimaging experiments. Garlic cloves were purchased from a local market and thoroughly cleaned to remove adhering impurities. Subsequently, 30 g of the peeled garlic cloves was homogenized in 70 mL of distilled water. The homogenate was filtered through qualitative filter paper, and the resulting filtrate was stored at 4 °C prior to further use [6] Purchased zebrafish feed (Shanghai Feixi Biotechnology Co., Ltd.) was then immersed in the garlic filtrate. After freeze-drying for 24 h in a freeze dryer, garlic-supplemented feed was obtained. During the experimental period, the test zebrafish were fed with 10 mg of the garlic-supplemented feed per individual daily for two consecutive days. Immediately after each feeding, a fasting protocol was implemented, and the fasting was maintained until the third day, after which the relevant physiological and biochemical indicators of the zebrafish were determined. Zebrafish in vivo imaging results in are detailed in **Figure S12**.

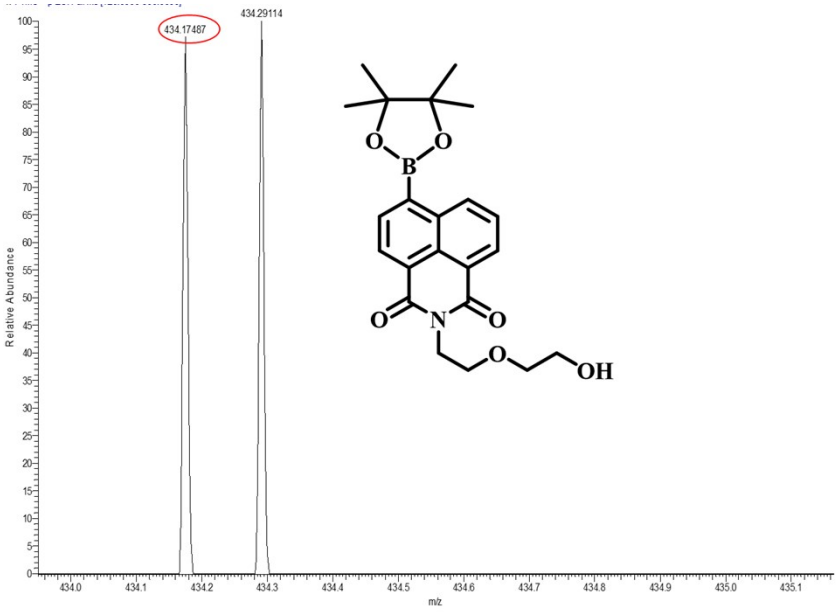

Figure S1. Mass Spectra of intermediate product A_1

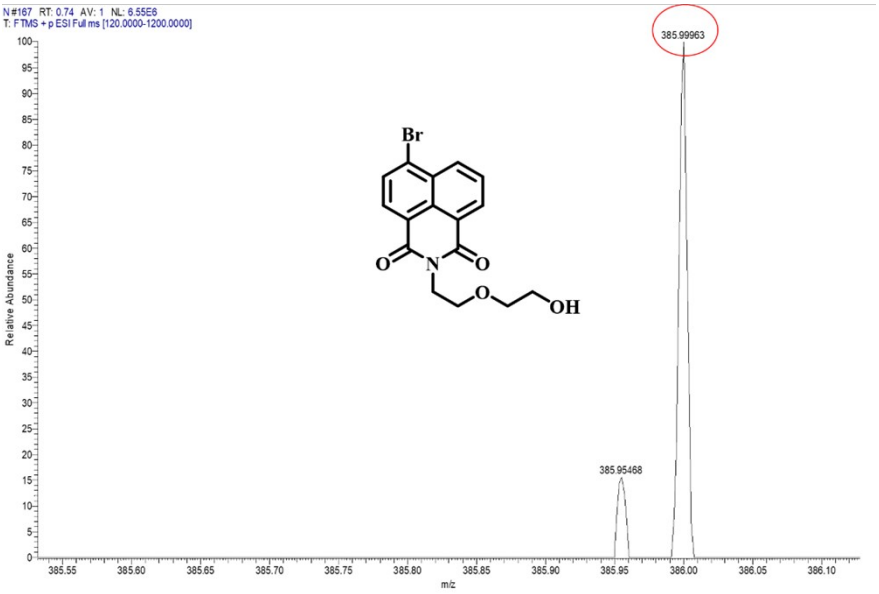

Figure S2. Mass Spectra of intermediate product A_2

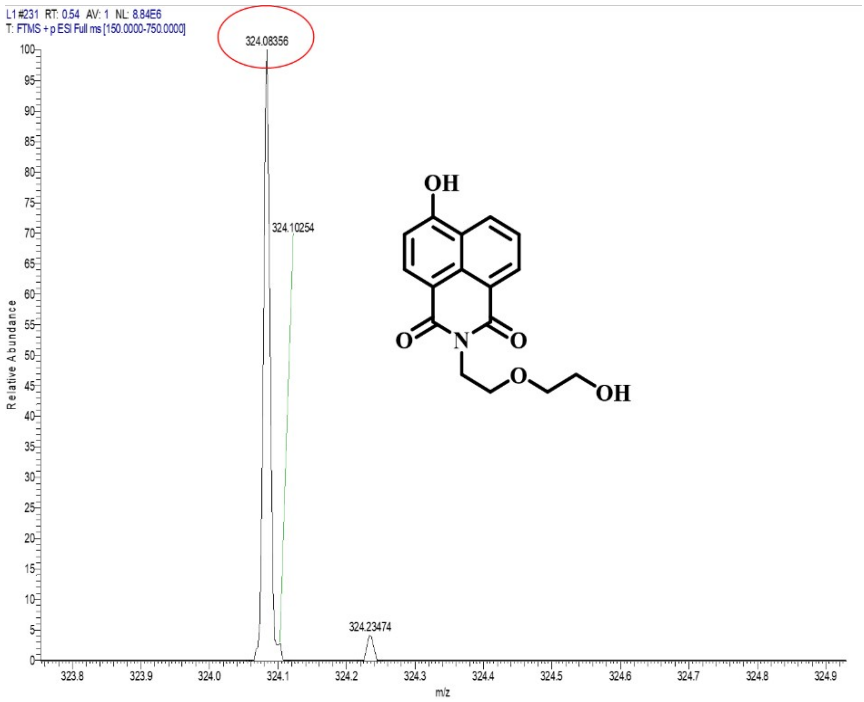

Figure S3. Mass Spectra of intermediate product A_3

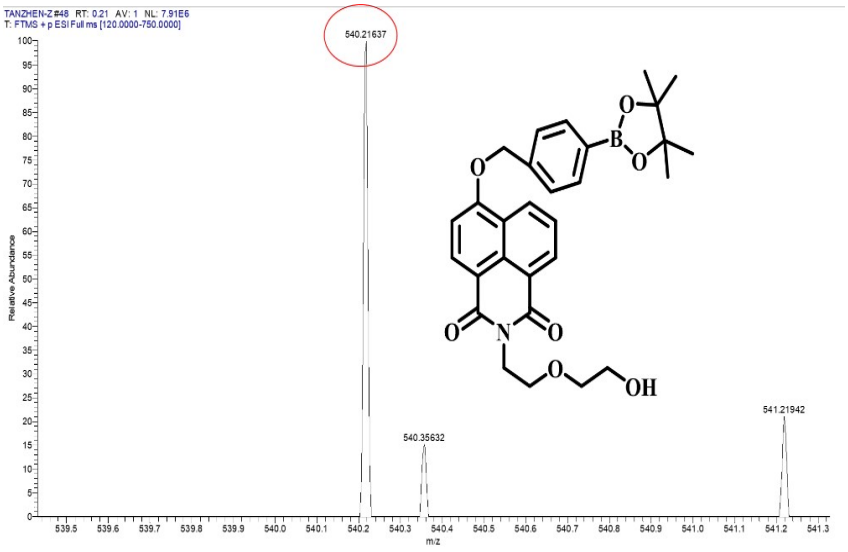

Figure S4. Mass spectra of the probe A

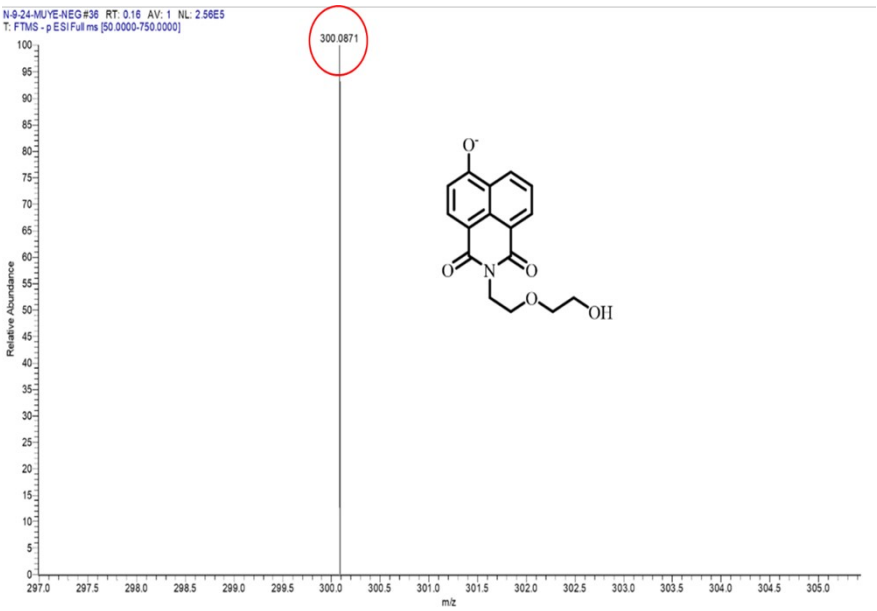

Figure S5. Mass spectra of the product formed by A and H_2O_2

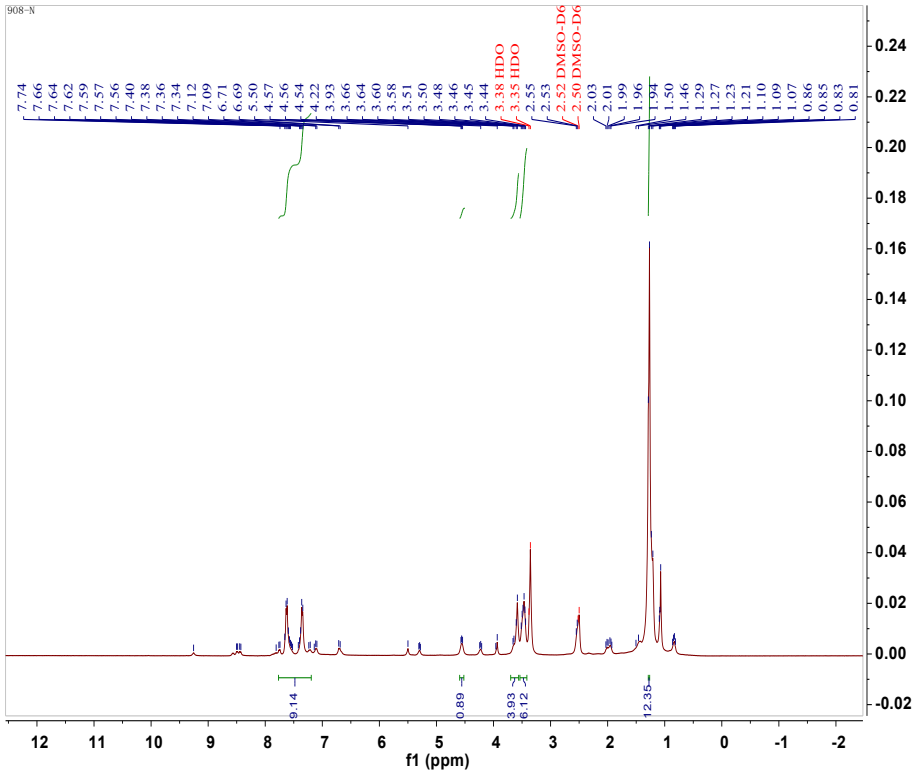

Figure S6. ^{1}H NMR spectrum of probe A in DMSO-d_6.

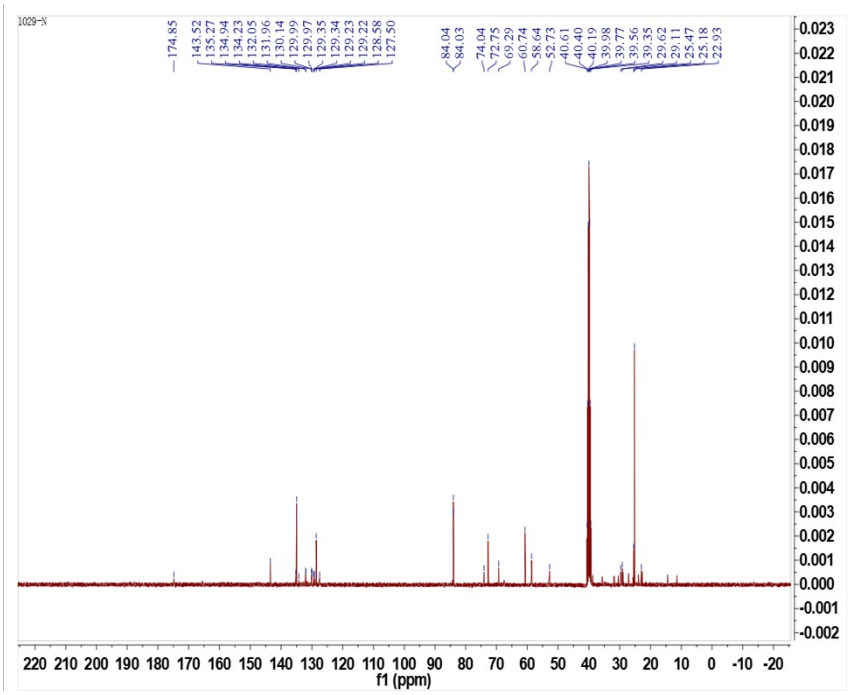

Figure S7. ^{13}C NMR spectrum of probe A in DMSO-d_6.

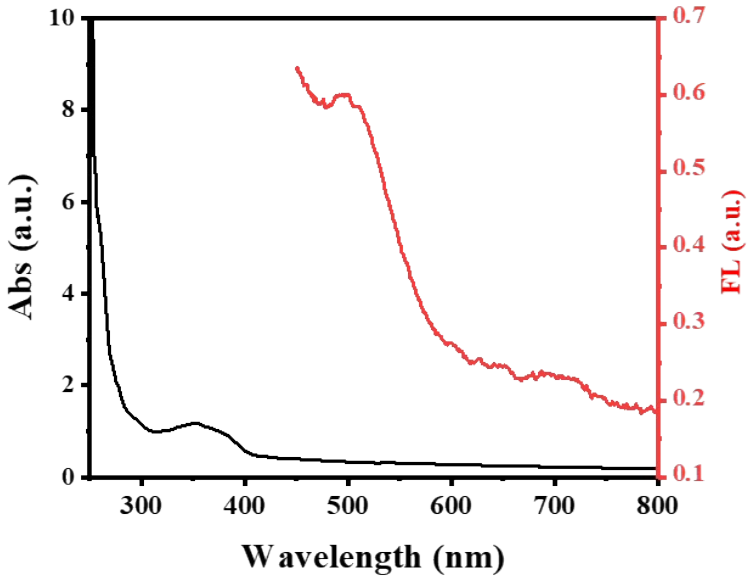

Figure S8. Fluorescence emission spectrum (red line) and UV-vis absorption spectrum (black line) of probe A.

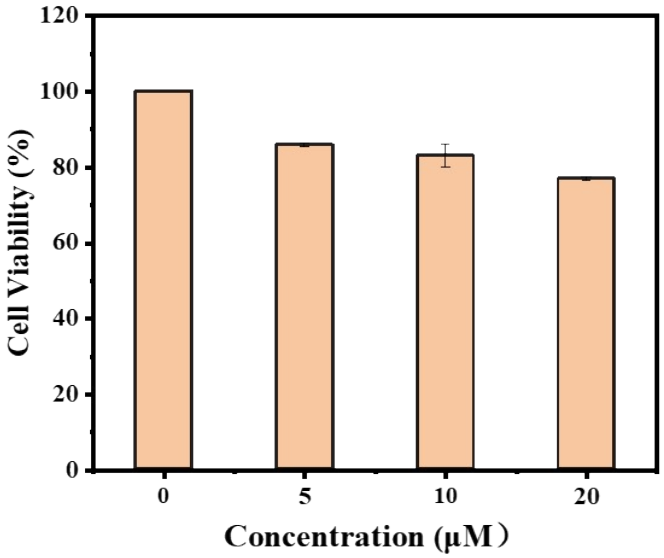

Figure S9. Effect of probe A on the survival of HeLa cells.

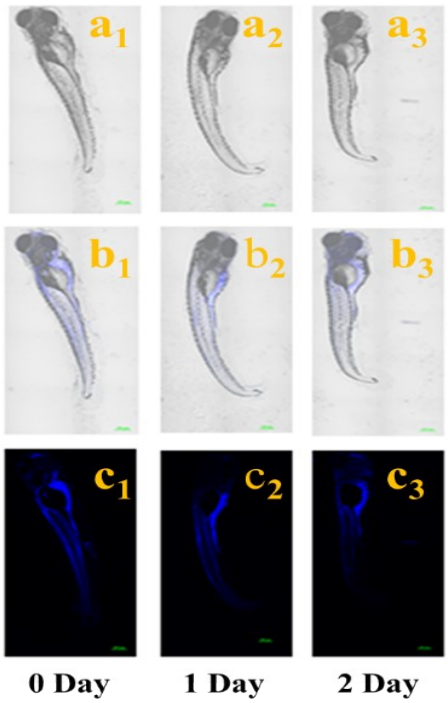

Figure S10. Confocal fluorescence microscopic images of zebrafish

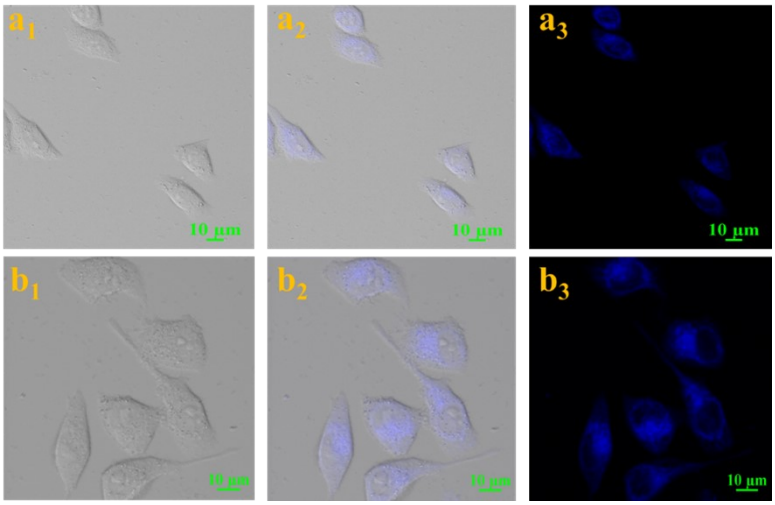

Figure S11. Confocal fluorescence microscopic images of HeLa cells. Probe B (10 μmol/L) with 90 μmol/L hydrogen peroxide for 30min (a_1-a_3), probe A (10 μmol/L) with 90 μmol/L hydrogen peroxide for 30min (b_1-b_3), Scale: 10 μm. Blue channel (λ_{em}=425-475 nm, λ_{ex}=402.9 nm).

As shown in figure S9, after probe A (10 μmol/L) (b_1-b_3) and probe B (10 μmol/L) (a_1-a_3) were incubated with hydrogen peroxide for 30 min, probe A showed stronger fluorescence than probe B. This show that probe A is more effective than probe B.

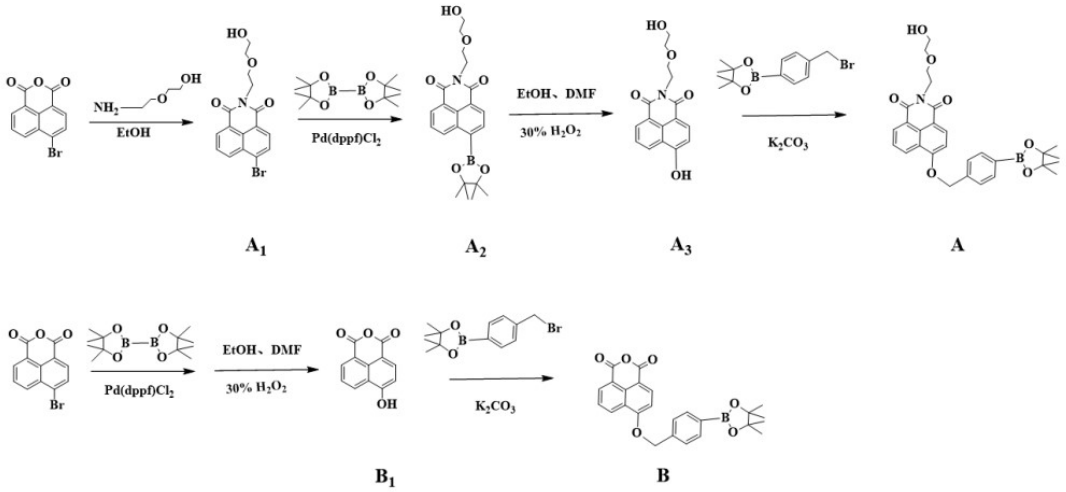

Figure S12. Different routes of probe a synthesis

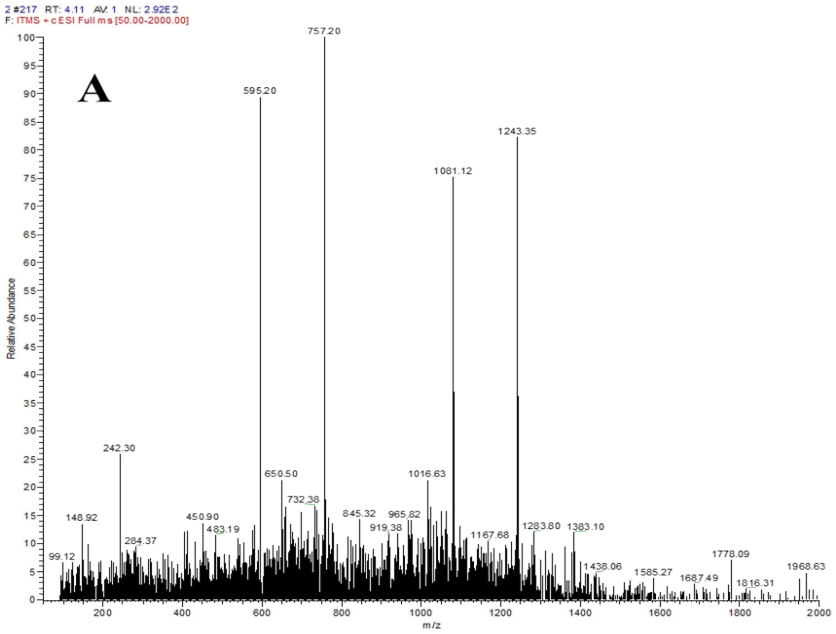
2 #217 RT: 4.11 AV: 1 NL: 2.92E2
F: ITMS + c ESI Full ms [50.00-2000.00]
A
757.20
595.20
1243.35
1081.12
242.30
650.50
1016.63
732.38
845.32
965.82
919.38
148.92
450.90
483.19
284.37
1167.68
1283.80
1383.10
99.12
1438.06
1585.27
1778.09
1687.49
1816.31
1968.63
Relative Abundance
m/z

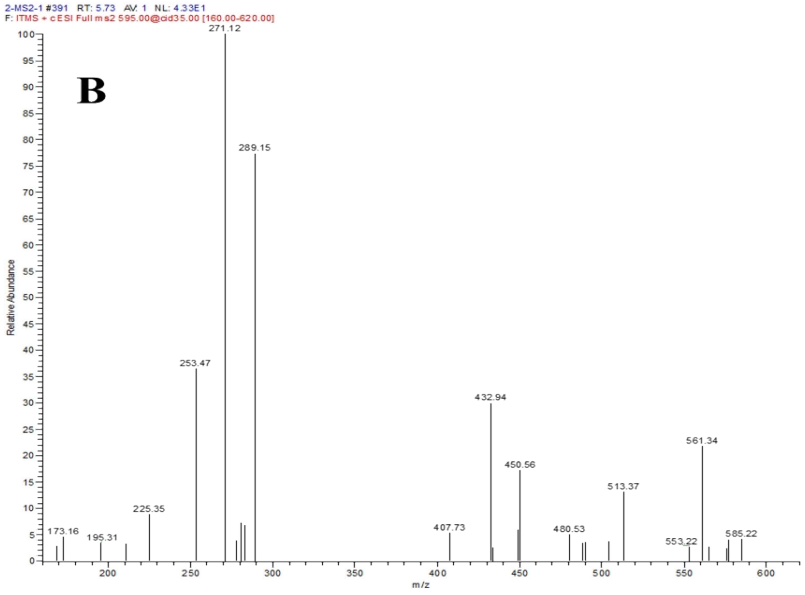
2-MS2-1 #391 RT: 5.73 AV: 1 NL: 4.33E1
F: ITMS + c ESI Full ms2 595.00@cid35.00 [160.00-620.00]
B
271.12
289.15
253.47
432.94
561.34
450.56
513.37
225.35
173.16
195.31
407.73
480.53
553.22
585.22
Relative Abundance
m/z

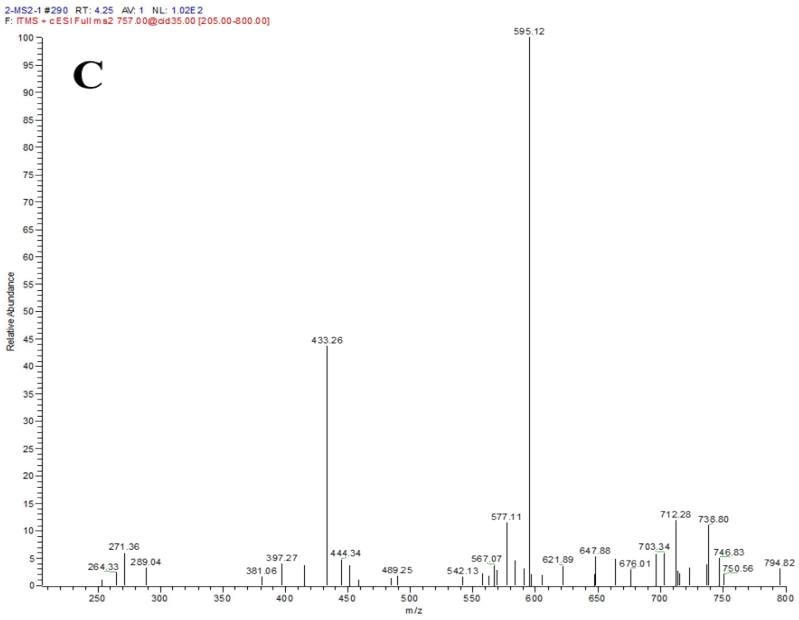

Figure S13. Mass Spectrometry of Garlic Saponins. (A) Garlic saponin+ESI primary mass spectrometry, (B) The secondary mass spectrum of the +ESI base peak 595 (m/z). (C)The secondary mass spectrum of the +ESI base peak 757 (m/z)

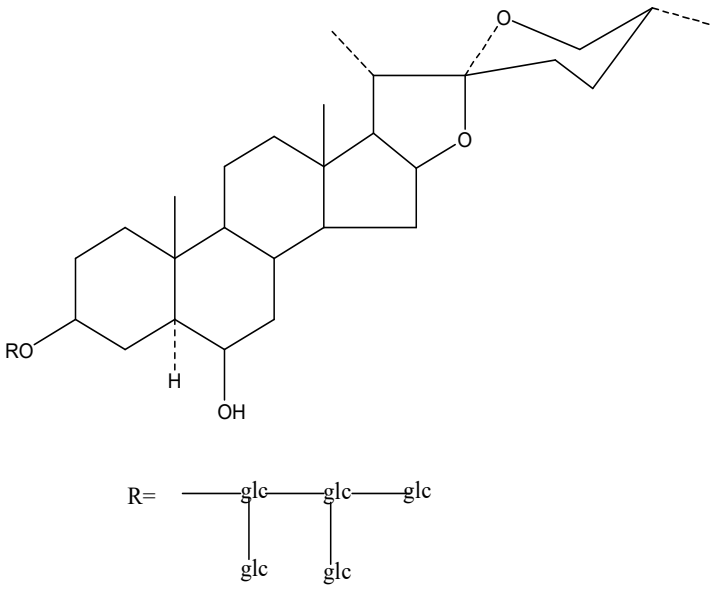

Figure S14. Structural diagram of Garlic saponin

Table S1. Atomic Orbital HOMO-LUMO Compositions of Compounds

Compound	HOMO(ev)*	LUMO(ev)*	⊿E(ev)
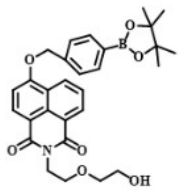	 E= **-7.56eV**	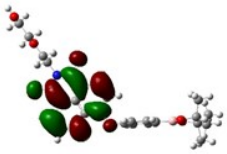 E= **-1.56eV**	6.00
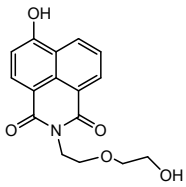	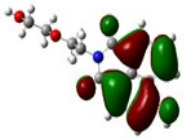 E= **-7.66eV**	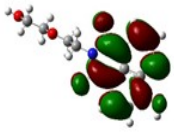 E= **-1.63eV**	6.03
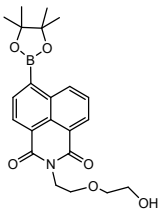	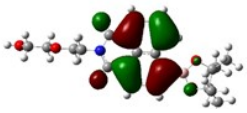 E= **-7.80eV**	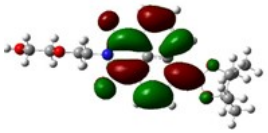 E= **-1.78eV**	6.02
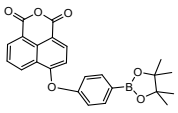	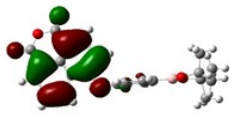 E= **-7.81eV**	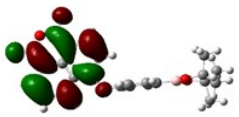 E= **-1.76eV**	6.05
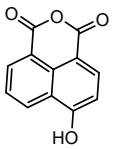	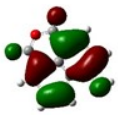 E= **-7.93eV**	 E= **-1.86eV**	6.07

*Note: All quantum chemical calculations were performed using the Gaussian 09/Gaussian 16 packages, with GaussView 6.0 software used for building the initial molecular structures and visualizing the calculation results. The classical B3LYP functional combined with the 6-31G(d,p) basis set was employed to perform full geometry optimizations of the target naphthalimide compounds in the gas phase/water phase.

Reference

(1) Nguyen, B.T.; Hong, H.T.; O'Hare, T.J.; Wehr, J.B.; Menzies, N.W.; Harper, S.M. A rapid and simplified methodology for the extraction and quantification of allicin in garlic. *J. Food Compos. Anal.* **2021**, 104, 104114. https://doi.org/10.1016/j.jfca.2021.104114.

(2) Yoon, S.A.; Oh, J.H.; Kim, S.K.; Lee, M.H. Water-sensitive ratiometric fluorescent probes and application to test strip for rapid and reversible detection of water. *Dyes Pigm.* **2019**, 165, 421-428. https://doi.org/10.1016/j.dyepig.2019.02.052.

(3) Solanki, P.; Kmin, S.A.; Manhas, A. Integrating machine learning with in silico studies and quantum chemistry: exploring novel compounds through multiscale screening targeting the CDK2 enzyme. *Comput. Biol. Med.* **2025**, 196, 110712. https://doi.org/10.1016/j.compbiomed.2025.110712.

(4) Sun, S.; Barnes, A. J.; Gong, X. X.; Lewis, R. J.; Dummer, N. F.; Bere, T.; Shaw, G.; Richards, N.; Morgan, D. J.; Hutchings, G. J. Lanthanum modified Fe-ZSM-5 zeolites for selective methane oxidation with H_2O_2. *Catal. Sci. Technol.* **2021**, 11, 8052-064. https://doi.org/10.1039/D1CY01643A.

(5) Zhang, Y. D.; Hu, H.; Song, L. M.; Liu, Z. H.; Ma, J. G.; Li, X. Y. Adverse effects of glyphosate and Microcystin-LR on fish health: evidence from structural and functional impairments in zebrafish gills. *Animals. (Basel).* **2025**, 15(16), 2355. https://doi.org/10.3390/ani15162355.

(6) Marić, P.; Ahel, M.; Maraković, N.; Lončar, J.; Mihaljević, I.; Smital, T. Selective interaction of microcystin congeners with zebrafish (Danio rerio) Oatp1d1 transporter. *Chemosphere* **2021**, 283, 131155. https://doi.org/10.1016/j.chemosphere.2021.131155.